

# Solution Equilibria in YbDOTMA, a Chiral Analogue of One of the Most Successful Contrast Agents for MRI, GdDOTA

Lorenzo Di Bari,<sup>[a]</sup> Guido Pintacuda,<sup>[b]</sup> and Piero Salvadori\*<sup>[a]</sup>

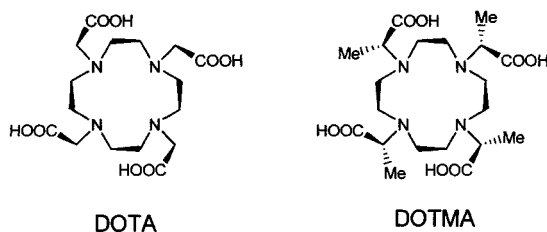
**Keywords:** Macrocyclic ligands / Conformational equilibria / EXSY spectroscopy / Lanthanide-induced shifts / Solution structure

The structure and the conformational equilibria in aqueous and methanolic solutions of YbDOTMA (DOTMA = (1*R*,4*R*,7*R*,10*R*)- $\alpha,\alpha',\alpha'',\alpha'''$ -tetramethyl-1,4,7,10-tetraazacyclododecane-1,4,7,10-tetraacetic acid) are investigated and the dynamics studied by means of NMR methods. The presence of two isomeric forms in slow exchange is confirmed and quantitatively characterized by EXSY. The exchange peaks are assigned to the inversion of the

conformation of the macrocycle ring. No evidence is obtained of a reorientation of the methyl acetate substituents. The protons switch between positions with the same geometrical factors, i.e. positions that would have the same pseudocontact shifts were it not for the different magnetic susceptibility anisotropies of the two species; steady-state NOE spectra on the major form allow unequivocal assignment of the conformations of the two isomers.

## Introduction

Macrocyclic octadentate ligands derived from a tetraazacyclododecane (cyclen) ring have received attention from several research groups as a result of their ability to form stable and nonlabile complexes with metal, mainly lanthanide, cations. In particular, one of the most successful ligands, DOTA<sup>[1]</sup> (Scheme 1), whose Gd<sup>III</sup> complex is widely used as a contrast agent in MRI and in biomedical applications, has been thoroughly investigated through the whole *f* transition.<sup>[2–9]</sup>



Scheme 1

More recently, chiral nonracemic derivatives and homologues of DOTA have also been synthesized and studied.<sup>[10–14]</sup> Among them, DOTMA (Scheme 1) is one of the most promising ligands because of the high relaxivity of its Gd complex.<sup>[15]</sup> Its crystal structure has been solved and some data reported, but the full set of coordinates is not yet available.<sup>[15]</sup> To our knowledge, no comprehensive study

of the dynamics in solution of DOTMA complexes has so far appeared in the literature although a preliminary report on YbDOTMA can be found in a MRI/MRS context.<sup>[14][16]</sup>

Chiral Ln<sup>3+</sup> complexes are expected to show optical activity of the lanthanide *f*–*f* transitions owing to the dissymmetrical crystal field the cation experiences. Indeed, preliminary results from a near-infrared (980 nm) circular-dichroism study of Yb complexes has been reported.<sup>[17]</sup> To understand the electronic spectroscopy of the lanthanide transitions, it is essential to have a clear picture of the structure in solution, particularly regarding the coordination polyhedron. Also, all the conformational rearrangements occurring at ordinary temperatures must be fully characterized. We undertook a thorough conformational and dynamical investigation of this molecule, making profit of a preliminary study due to Brittain and Desreux<sup>[10]</sup> and of the huge amount of work on DOTA-like molecules.<sup>[2–9]</sup>

The solid-state X-ray characterization of Ln<sup>3+</sup> complexes with DOTA analogues reveals that the eight coordination sites, four nitrogens and four oxygens, provided by these ligands, are arranged in two parallel squares, tilted by an angle  $\varphi$  (Figure 1). According to the value of this angle the coordination polyhedron can range from a perfect anti-prism ( $\varphi = 45^\circ$ ) to a prism ( $\varphi = 0^\circ$ ). Neither limiting case has been observed so far in the crystal structures and most known geometries cluster around two values:  $\varphi = 15^\circ$  and  $30^\circ$ . For example, LnDOTA (Ln = Eu,<sup>[3]</sup> Gd,<sup>[5]</sup> Lu<sup>[7]</sup>) and the Eu-phenylethyl amide synthesized by Parker<sup>[11]</sup> belong to the latter group; to the former can be assigned LaDOTA,<sup>[9]</sup> LaDOTAM,<sup>[18]</sup> EuTHP,<sup>[19]</sup> YDOTPBz<sub>4</sub><sup>[20]</sup> and Parker's Eu-naphthylethyl amide.<sup>[12]</sup>

These two structures actually correspond to two main internal degrees of freedom. One, concerning the conformation of the ring (Figure 1a), can assume two forms referred to as ( $\delta\delta\delta\delta$ ) and ( $\lambda\lambda\lambda\lambda$ ),<sup>[21]</sup> which are in enantiomeric relation. The other involves the rotation about the N–C $\alpha$  bond (Figure 1b), switching the substituent residue between

<sup>[a]</sup> Centro di Studio del CNR per le Macromolecole Stereoordinate ed Otticamente Attive, Dipartimento di Chimica e Chimica Industriale, Via Risorgimento 35, I-56126 Pisa, Italy  
Fax: (internat.) + 39(050) 918260  
E-mail: psalva@dccl.unipi.it

<sup>[b]</sup> Scuola Normale Superiore, Piazza dei Cavalieri 7, I-56126 Pisa, Italy  
Supporting information for this article is available on the WWW under <http://www.wiley-vch.de/home/eurjic> or from the author.

two *gauche* conformations. This induces a sign change in the distortion of the coordination polyhedron, named as  $\Delta$  or  $\Lambda$ .

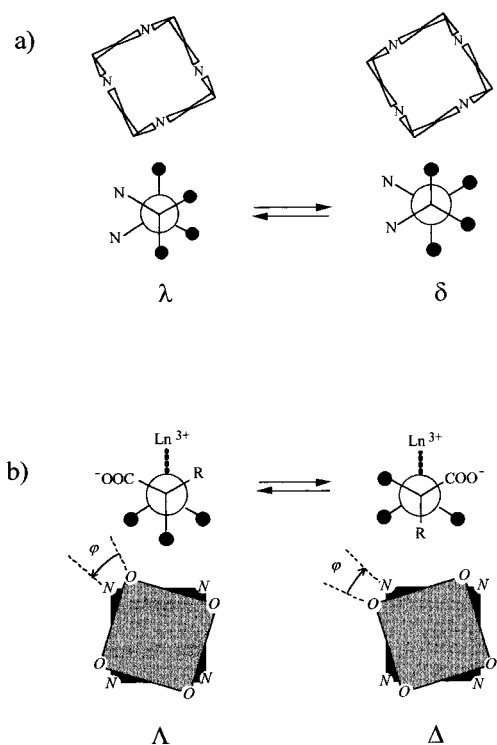
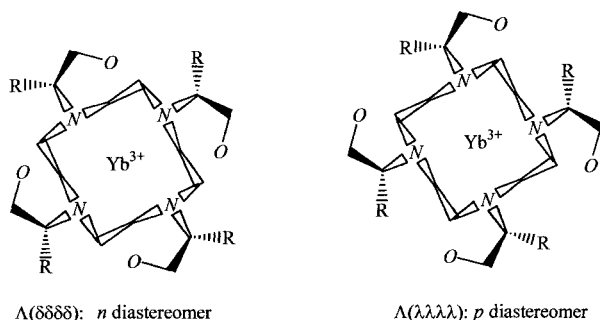


Figure 1. a) Equilibria between the  $\delta$  and  $\gamma$  forms of the cyclen ring. The Newmann projection is referred to the bond connecting two ethilenic carbons of the macrocycle; the black circles represent the hydrogen atoms; b) equilibria between the  $\Delta$  and  $\Lambda$  conformation of the cyclen side-arms in the DOTA-type complexes with  $\text{Ln}^{(\text{III})}$ . The Newmann projection refers to the bond between the acetate  $\text{C}^\alpha$  and the nitrogen; the black circles represents the hydrogen atoms and  $\text{R} = \text{H}, \text{Me}$  (DOTA and DOTMA, respectively). On the bottom, a schematic representation of the coordination polyhedron is depicted: at the corners of the light gray squares are the oxygens and at the corners of the dark ones the nitrogen atoms (the water molecule possibly axially coordinated is not indicated).

The two descriptors can be alike or different, e.g.  $\Lambda(\lambda\lambda\lambda\lambda)$  or  $\Lambda(\delta\delta\delta\delta)$ , giving rise to a diastereomeric pair *p* or *n*, respectively (Scheme 2,  $\text{R} = \text{H}, \text{Me}$ ).<sup>[22]</sup> A further relevant parameter to take into account is the orientation of the carboxylate bond, which is less accessible to experimental determination via NMR spectroscopy.



Scheme 2

The two diastereoisomeric forms *n* and *p* show a different arrangement of the oxygen atoms, in order to preserve the  $\text{Ln}-\text{O}$  distances at a value of about 2.4 Å. Accordingly, a less distorted ( $\varphi = 15^\circ$ ) coordination polyhedron corresponds to the *p* diastereomer, while the *n* diastereomer has a much more distorted ( $\varphi = 30^\circ$ ) structure.<sup>[4][8]</sup>

Most complexes have also been structurally characterized in solution, often using the paramagnetic character of the metal centre.<sup>[2-4,6,8,10]</sup> While in most cases there is no evidence of structural equilibria and X-ray geometries possibly reflect the most likely conformation in solution, the complexes of DOTA reveal an intriguing network of solution equilibria, which have been studied by various NMR techniques, with reference to limiting crystal geometries. In particular, Aime and co-workers pointed out that the ratio of populations of *n* and *p* types varies along the lanthanide series<sup>[4]</sup> and that superimposed on the conformational change, there is a hydration–dehydration equilibrium,<sup>[8]</sup> whose position depends on the size of the central ion.<sup>[4]</sup>

The pseudocontact shifts of  $\text{YbDOTA}$ <sup>[10]</sup> reveal that the two sets of signals for the two forms are proportional. This means that the sets of geometrical factors of the protons in the two forms are equal. This does not necessarily mean that *each* proton occupies a position characterized by the *same* geometrical factor in the two forms, since there can be a pairwise proton-swap between equivalent sites. In 1992, Aime and co-workers<sup>[4]</sup> assigned the two spectra to two *different* structures, corresponding to the diastereomeric pair *p* and *n*. Indeed, they demonstrated the occurrence of such a rearrangement through EXSY measurements, as discussed in ref.<sup>[4]</sup> and ref.<sup>[6]</sup> and below. However, no positive evidence of the assignment of the *n* structure to the major component of  $\text{YbDOTA}$  in solution can be found in the pseudocontact shifts. In the present work, to our knowledge for the first time, we use such a simple experiment as a monodimensional NOE measurement to assign unequivocally the structure of the major isomer.

The presence of a stereogenic centre on the side arm in DOTMA complicates the equilibrium network, since, for instance, the two forms  $\Lambda(\lambda\lambda\lambda\lambda)$  and  $\Delta(\delta\delta\delta\delta)$  are no longer equivalent. The intrinsic chirality of the ligand is shown to induce a preference in the distortion of the coordination polyhedron, which in the present work is demonstrated to be  $\Lambda$ . This finding is essential in understanding the chiroptical properties of  $\text{YbDOTMA}$ .

## Results

The spectrum of  $\text{YbDOTMA}$  in water, as discussed by Brittain and Desreux,<sup>[10]</sup> shows that the complex is present in solution in two forms '*D*' and '*d*' in slow exchange, characterized by different anisotropy factors  $D_D$  and  $D_d$  and different signal intensities, by analogy with  $\text{YbDOTA}$ .<sup>[4]</sup> However, unlike in DOTA, here the less populated form has the larger value of the *D* factor. We can observe that the spectra of the two forms are exactly proportional (isomorphic), as demonstrated in Figure 2, and

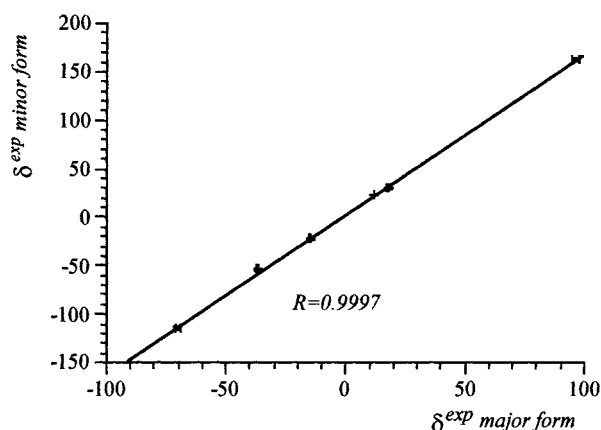


Figure 2. Correlation plot between the experimental  $\delta^{\text{exp}}$  values of the major (D) and minor (d) forms of YbDOTMA in  $\text{D}_2\text{O}$ .

only the large difference between the anisotropy factors,  $D_{\text{D}}$  and  $D_{\text{d}}$ , justifies the appearance of two distinct sets of signals for the two isomers. It follows that, at least in principle, the two spectra can be associated with the same molecular structure. Alternatively, two conformations must be found bearing the protons in positions characterized by very similar geometrical factors.

Following Brittain and Desreux,<sup>[10]</sup> a set of suitable parameters for the spectral assignment can be produced from the coordinates of GdDOTA<sup>[5]</sup> [we chose to start from the  $\Lambda(\delta\delta\delta\delta)$  form]. Since the spectrum is compatible with a  $C_4$  symmetry, the analysis of the pseudocontact shifts involves only a linear fitting of one parameter (of the anisotropy  $D$ ). The geometry factors for sets of equivalent protons were averaged in order to compensate for the lower symmetry of the crystal structure.<sup>[23]</sup> The pro- $R$  hydrogen on each acetate arm

was replaced by a methyl group with standard bond lengths and angles. The methyl acetate arm was then systematically rotated around the  $\text{N}-\text{C}^\alpha$  bond to obtain the best agreement<sup>[24]</sup> between the geometrical factors and the observed pseudocontact shifts, finding an optimal value of the torsion angle  $\text{YbNC}^\alpha\text{M}$  of about  $167^\circ$  (which corresponds to a coordination geometry of  $\Lambda$ -type). The carboxylate was then rotated to restore the distance  $\text{Yb}-\text{O}$  of 2.4 Å, but this had no effect on the proton geometrical factors.

In such a way, a full set of satisfactory geometrical parameters and the relative structure were obtained. It should be observed that the solution of this optimization is unique, which excludes a rotation of the methyl acetate as the origin of the two forms, in agreement also with other findings on similar structures.<sup>[13]</sup>

An equivalent set was provided by the following stereochemical operations on these structures: (i) mirror image (inversion) of the whole complex; (ii) epimerization of the four  $\text{C}^\alpha$  stereocentres (these operations must be followed again by the carboxylate rotation). The result was once more a ( $RRRR$ )-YbDOTMA, but the arrangement of the macrocyclic ring is opposite. In other words, the tetraazacyclododecane shifts from a  $(\lambda\lambda\lambda\lambda)$  to a  $(\delta\delta\delta\delta)$  conformation. Obviously, starting from the  $\Lambda(\lambda\lambda\lambda\lambda)$  form of GdDOTA, one would obtain first the  $\Lambda(\lambda\lambda\lambda\lambda)$  isomer and, after the formal inversion and epimerization, the other. The two sets of geometrical factors for the cyclen ring are obviously equal. For the methyl group and for the CH such equality does not follow by necessity; however, the difference between the geometrical factors calculated for the two forms is less than 10%. Any attempt to use this small difference for structural assignment is nullified by the proportionality of the spectra of the two species. Furthermore, smaller geo-

Table 1. Experimental and calculated lanthanide-induced NMR shifts ( $\delta$ , in ppm) of the major and minor YbDOTMA species in  $\text{D}_2\text{O}$  and MeOD ( $T = 25^\circ\text{C}$ ). The factors in the second column are calculated on a structure derived, as described in the text, from GdDOTA<sup>[5]</sup> (see also Table 4); induced chemical shifts are relative to diamagnetic LuDOTA (as far as it concerns the ring protons and the acetate one) and to a value of  $\delta = 0.9$  for the case of the methyl resonance.

proton	$\frac{(3 \cos^2 \theta_i - 1)}{r_i^3} \cdot 10^2$	major form (in-type, $p$ diastereomer)				minor form (M-type, $n$ diastereomer)				
		$\text{D}_2\text{O}$		MeOD		$\text{D}_2\text{O}$		MeOD		
		$\delta^{\text{exp}}$	$\delta^{\text{calc}}$	$\delta^{\text{exp}}$	$\delta^{\text{calc}}$	$\delta^{\text{exp}}$	$\delta^{\text{calc}}$	$\delta^{\text{exp}}$	$\delta^{\text{calc}}$	
axial <sub>1</sub>	3.09	A <sub>1</sub>	94.3	94.0	109.9	109.8	a <sub>1</sub>	160.9	159.9	179.9
axial <sub>2</sub>	-0.942	A <sub>2</sub>	-38.9	-35.1	-41.1	-38.2	a <sub>2</sub>	-55.9	-53.9	-61.0
equatorial <sub>1</sub>	0.502	E <sub>1</sub>	10.5	11.1	14.5	14.8	e <sub>1</sub>	22.2	22.7	25.8
equatorial <sub>2</sub>	0.652	E <sub>2</sub>	16.3	15.9	20.5	20.3	e <sub>2</sub>	28.7	30.6	32.8
acetate <sup>c</sup>	-2.16	C	-72.5	-74.2	-81.8	-82.9	c	-117.4	-118.5	-133.9
methyl <sup>c</sup>	-0.407	M	-16.0	-18.0	-16.8	-18.6	m	-23.2	-25.6	-25.6
$R^a$ %			3		2		2		2	
$D^b$			3200±90		3700±50		5300±100		6000±150	

<sup>[a]</sup> Nonweighted agreement factor; see ref.<sup>[23]</sup> – <sup>[b]</sup> Magnetic anisotropy factor, in units of  $[\text{ppm} \text{ \AA}^3]$ . – <sup>[c]</sup> Average between the values found in the two forms obtained as described in the text, (-2.09 and -2.23 for C; -0.423 and -0.391 for M in the major and minor form, respectively).

metrical adjustments<sup>[4]</sup> may account for minor improvements of the agreement factors.

In such a way, a full set of satisfactory geometrical parameters and two relative structures were obtained (see Table 1 and Figure 3).<sup>[25]</sup> The coordination geometry is of  $\Lambda$  type in both cases, with the same torsion angles around the N–C $\alpha$  bond; only the arrangement of the macrocycle is opposite.

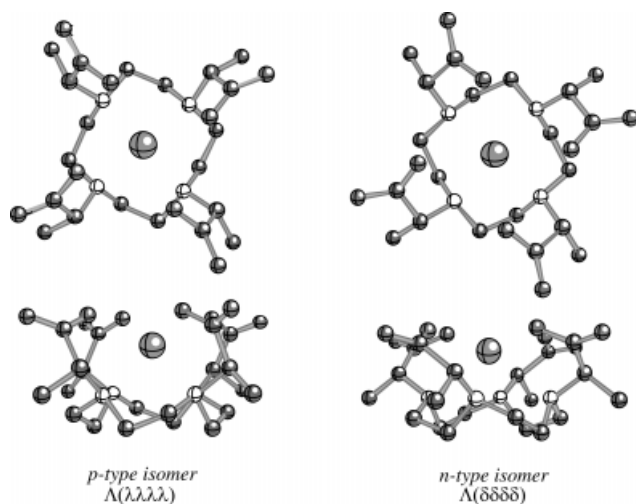


Figure 3. Two isomeric structures of YbDOTMA compatible with the observed proton paramagnetic shifts. On the left a  $\Lambda(\lambda\lambda\lambda\lambda)$  conformation is displayed, on the right a  $\Lambda(\delta\delta\delta\delta)$  one. They have been assigned to the major and minor form, respectively.

In order to determine the thermodynamic parameters for the isomerization equilibrium, a variable-temperature study was undertaken. On increasing the temperature, the signals of the minor form become comparatively smaller, which indicates a negative enthalpy for this process. We recorded the spectra in methanol as well, in order to cover a broader temperature range. Indeed, the spectrum in this solvent is very similar to that in water reported in Table 1; once more two forms are present, whose resonances can be predicted with the same geometrical factors used above. The two anisotropy factors are of the same order of magnitude as those found in water and their ratio seems solvent independent. Furthermore, in methanol the minor form is slightly more populated at room temperature than in water ( $D/d = 14.2$  and  $20$ , respectively). The main difference between the two solvents is that in MeOD the resonances of the counterion, *N*-methylglucammonium, which are strongly concentration and temperature dependent, are clearly visible, downfield shifted. Therefore, we can conclude that the cation is at least partly bound in methanol, while it is not in D<sub>2</sub>O. The downfield shift shows that it lies axially above or below the metal centre, similar to recently reported for phosphonate systems.<sup>[26]</sup>

On recording variable temperature spectra in MeOD between  $-80$  and  $60^\circ\text{C}$  one observes a migration of all the signals according to the variation of  $D$ , predicted by Ble-

aney.<sup>[27]</sup> Unfortunately, the values collected in Table 2 do not allow  $1/T$  and  $1/T^2$  dependences to be unambiguously distinguished. Furthermore, at low temperature, all the lines become broader, owing to faster transverse relaxation.

Table 2. Temperature variation of the anisotropy susceptibility parameter  $D$  of the major form of YbDOTMA and of the equilibrium constant  $K$  between the two isomers.

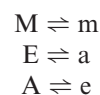
temperature ( $^\circ\text{C}$ )	$D$ ( $\pm 100$ )	$\frac{[d]}{[D]}$ %
60	3180	6.55
25	3490	7.0
0	3770	8.1
-25	4025	9.6
-50	4450	12.0
-80	5070	14.2

The persistence of signals of the minor form up to  $60^\circ\text{C}$  could be observed, although at this temperature they appear very broadened. In fact, they start to coalesce with those of the major form, because of the faster equilibrium and of the smaller spectral width, which implies more stringent requirements for the slow exchange limit.

Integration of the signals of the methyl in the two forms afforded an estimation of the temperature dependence of the equilibrium constant,  $K$ , shown in Table 2. This gave the thermodynamic parameters in methanol:  $\Delta H_s^0(\text{M}) = -4.0 \pm 0.9 \text{ kJ mol}^{-1}$  and  $\Delta S_s^0(\text{M}) = -35.4 \pm 0.5 \text{ J K}^{-1} \text{ mol}^{-1}$ . In D<sub>2</sub>O, the temperature range that can be covered goes from  $0$  to  $50^\circ\text{C}$ , because above this limit the signals of the minor form become exceedingly broad. In water, the following values were found:  $\Delta H_s^0(\text{W}) = -8 \pm 2 \text{ kJ mol}^{-1}$  and  $\Delta S_s^0(\text{W}) = -50 \pm 10 \text{ J K}^{-1} \text{ mol}^{-1}$ .

The dynamics of the interconversion between the two forms has been investigated through two-dimensional exchange spectra (EXSY) at variable mixing time in water and in methanol at  $25^\circ\text{C}$ .

From inspection of Figure 4, we observe the following equilibria, with reference to the notation of Table 1:



while there is no evidence of exchange within the major or the minor form [e.g.,  $\text{E} \rightleftharpoons \text{A}$ ], either between equatorial or axial protons of the two forms [e.g.,  $\text{E} \rightleftharpoons \text{e}$ ]. Therefore, we can conclude that the isomerization process involves a ring inversion, exchanging the macrocycle hydrogens between positions characterized by pairwise equal geometrical factors. Such an observation is in perfect agreement with the structure pair determined above and depicted in Figure 3. Unfortunately, following their construction, it is impossible to assign either of the two to the major or minor component.

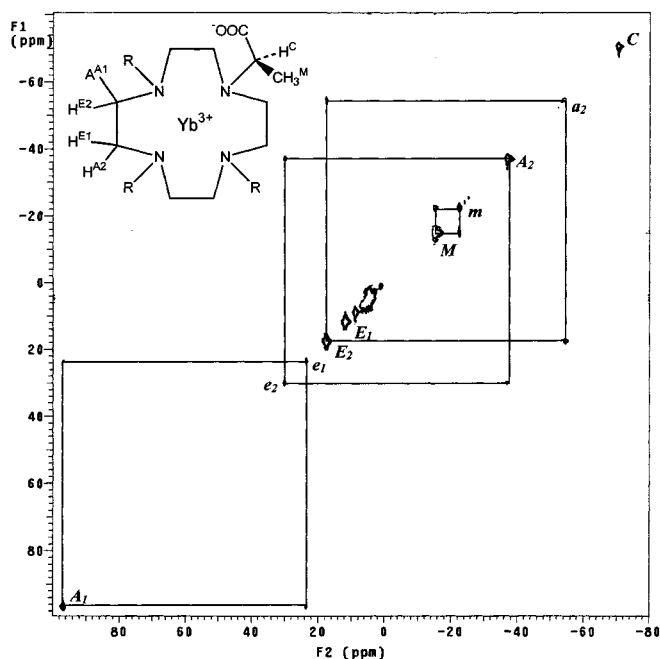


Figure 4. Proton labelling and EXSY spectrum of YbDOTMA at 25°C in D<sub>2</sub>O (within -80 and 100 ppm). Upper and lower case letters refer to the major and minor forms resonances, respectively.

To this end, steady-state NOE<sup>[28]</sup> spectra were recorded between selected protons of the molecule (see Supporting Material). When the resonance at  $\delta = -70.4$ , due to the methyl acetate methyn proton C, is irradiated, an intense enhancement of E<sub>2</sub> is observed, while no effect is detected on E<sub>1</sub>; at the same time, on saturating A<sub>2</sub>, C is enhanced. The interpretation of these data is discussed in the next section.

A quantitative evaluation of EXSY spectra at variable mixing time,  $\tau_m$ , allowed us to assess the dynamic constant for the observed kinetic process. Direct analysis, as de-

scribed by Perrin and Gipe,<sup>[29]</sup> of the integrated intensity matrix,  $\mathbf{A}(\tau_m)$  for a given  $\tau_m$  gives the dynamic matrix,  $\mathbf{L}$ ,

$$\mathbf{L} = \frac{1}{\tau_m} \ln(\mathbf{P}^{-1}\mathbf{A}) = \frac{1}{\tau_m} \mathbf{U}^{-1} \ln(\mathbf{A}) \mathbf{U} \quad (1)$$

where  $\mathbf{U}$  is the matrix of eigenvectors and the diagonal matrix  $\mathbf{\Lambda}$  contains the eigenvalues,  $\{\Lambda\}_{ii}$ , of  $\mathbf{P}^{-1}\mathbf{A}$ . The diagonal matrix  $\mathbf{P}$  contains the relative populations of the exchanging species,<sup>[30]</sup> so that the elements of  $\mathbf{P}^{-1}\mathbf{A}$  are the normalized amplitudes of the peaks.

We repeated the experiment with different mixing times, ranging from 5 to 30 ms, and we measured the integral of the methyl signals in the two forms and of the cross peaks between them, as reported in Table 3.

Cross relaxation gives only a negligible contribution to the cross-peak amplitudes at the very short  $\tau_m$  used in our experiments, hence the off-diagonal elements of  $\mathbf{L}$  are  $L_{ij} = -k_{ij}$ , where  $k_{ij}$  is the first-order rate constant for the exchange from site  $i$  to site  $j$ . Equation (1) then gives the rates, also shown in Table 3, whose average value is  $6.3 \pm 0.8 \text{ s}^{-1}$  for the D  $\rightarrow$  d process and  $136 \pm 16 \text{ s}^{-1}$  for the reverse in water, whereas, for the same processes in methanol one finds  $6.9 \pm 0.6 \text{ s}^{-1}$  and  $93 \pm 4 \text{ s}^{-1}$ , respectively.<sup>[31]</sup> These values seem to be quite reliable, since the ratio between the two constants in water [ $k_{dD}/k_{Dd} = 21.6$ ] is in agreement with the relative concentrations of the two isomers (major/minor = 20 under our experimental conditions) and the same holds true in methanol, as well. We can observe that the dynamics in the two solvents are very similar, which justifies our extrapolation of the thermodynamic data obtained in methanol to water.

## Discussion

The possible solution equilibria in YbDOTMA can be represented, by analogy with YbDOTA,<sup>[8]</sup> as in Figure 5.

Table 3. Integrated intensity matrix for the exchange of the signals of the methyl group in water and in methanol. The index 1 represents the resonance frequency of M and 2 the one of m, so that  $I_{11}$  and  $I_{22}$  are the intensities of the diagonal peaks of the forms D and d, while  $I_{12}$  and  $I_{21}$  are the intensities of the cross-peaks, all normalized to  $I_{11} = 100$ .

D <sub>2</sub> O:	$\tau = 5\text{ms}$	$\tau = 10\text{ms}$	$\tau = 20\text{ms}$	$\tau = 30\text{ms}$
$\begin{pmatrix} I_{11} & I_{12} \\ I_{21} & I_{22} \end{pmatrix}$	$\begin{pmatrix} 100 & 2.26 \\ 2.27 & 2.78 \end{pmatrix}$	$\begin{pmatrix} 100 & 4.40 \\ 4.70 & 1.72 \end{pmatrix}$	$\begin{pmatrix} 100 & 4.19 \\ 4.73 & 0.69 \end{pmatrix}$	$\begin{pmatrix} 100 & 4.72 \\ 5.32 & 0.33 \end{pmatrix}$
$k_{mM} (\text{M}^{-1}\text{s}^{-1})$	6.00	7.47	5.32	6.38
$k_{Mm} (\text{M}^{-1}\text{s}^{-1})$	120.89	159.28	120.11	143.93
MeOD:	$\tau = 10\text{ms}$	$\tau = 20\text{ms}$	$\tau = 30\text{ms}$	
$\begin{pmatrix} I_{11} & I_{12} \\ I_{21} & I_{22} \end{pmatrix}$	$\begin{pmatrix} 100 & 5.1 \\ 6.4 & 5.4 \end{pmatrix}$	$\begin{pmatrix} 100 & 6.7 \\ 6.6 & 1.5 \end{pmatrix}$	$\begin{pmatrix} 100 & 7.8 \\ 8.4 & 1.4 \end{pmatrix}$	
$k_{mM} (\text{M}^{-1}\text{s}^{-1})$	6.33	7.69	6.61	
$k_{Mm} (\text{M}^{-1}\text{s}^{-1})$	98.17	93.61	88.08	

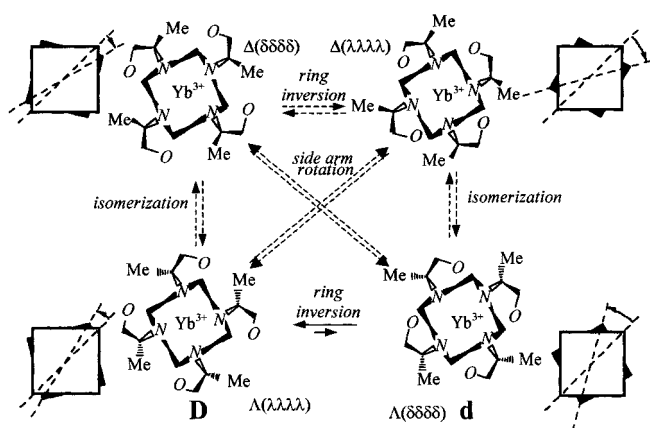


Figure 5. Schematic representation of the structure and dynamics of the diastereomers of YbDOTMA complexes. The conformation of the chelate systems and the coordination polyhedron are depicted. Following the interconversion between the major and minor forms, a different distortion of the coordination polyhedron is forced in the two forms, as discussed in the text.

The exchange processes in the rows are due to an inversion of the macrocyclic ring, while those on diagonals rely upon a rotation of the methyl acetate arms. In the columns, the two motions occur simultaneously (and possibly concertedly). On the left the *p* diastereomers are presented, on the right the *n*. In the case of DOTA, the two forms along each column are optical antipodes, whereas for DOTMA, the presence of the stereogenic centres at the C<sup>α</sup> makes them diastereomers. Although this is only a crude representation, it shows that in the two rows the coordination polyhedra are distorted antiprisms with opposite tilt angles. Clearly, since DOTA is achiral, the sign of such a distortion is irrelevant (it cannot be defined on a macroscopic level).

The populations of all the four DOTMA structures must be expected to be different. Indeed, only two species could be identified in the one-dimensional <sup>1</sup>H-NMR spectrum, in largely different amounts; both have  $\Lambda$  conformation of the side arm, bearing the methyl group *anti* with respect to N–Yb<sup>III</sup>. The excellent agreement of the chemical shifts with geometrical factors derived from a crystal structure rules out any fast motion and confirms the substantial rigidity of the chelate systems already reported in the literature.<sup>[4]</sup> We have observed that there is no evidence of a rotation of the methyl acetate arm, which amounts to saying that only one of two rows of Scheme 1 is populated and therefore that only one equilibrium is present in solution for YbDOTMA, between the  $\Lambda(\lambda\lambda\lambda\lambda)$  and  $\Lambda(\delta\delta\delta\delta)$  forms.

On the basis of the paramagnetic shifts (as well as the Yb-proton distances and therefore of Curie relaxation rates) it is not possible to assign either of the two conformations to the minor or major isomer; in contrast, the NOE spectra allow one to assign unequivocally the structure of the major isomer to one of the two conformations. In effect, the neat NOE between the C and E<sub>2</sub> protons cannot be justified for an *n*-type structure, since the two protons are far apart (3.35 Å). On the contrary, in the *p*-type the interproton distance is only 2.55 Å.<sup>[32]</sup> We can conclude that the  $\Lambda(\delta\delta\delta\delta)$  conformation must be assigned to the minor

isomer and the  $\Lambda(\lambda\lambda\lambda\lambda)$  to the major one, as depicted in Figure 3; the relevant parameters of such geometries are shown in Table 4. It must be stressed that, in reverse analogy with YbDOTA, the metal ion is more buried in the major form in the case of YbDOTMA.

Table 4. Conformation and relevant atomic distances [Å] and angles in the two isomers of YbDOTMA. The geometries were obtained from the X-ray data of GdDOTA (ref.<sup>[5]</sup>), according to the procedure described in the text.

	major form	minor form
	$\Lambda(\lambda\lambda\lambda\lambda)$	$\Lambda(\delta\delta\delta\delta)$
O–O	3.07	3.19
N–N	2.97	2.97
Yb–O	2.48	2.48
Yb–plane(O <sub>4</sub> )	1.01	0.72
Yb–N	2.66	2.66
Yb–plane(N <sub>4</sub> )	1.63	1.63
twist angle ( $\varphi$ )	17°	40°
YbNC <sup>α</sup> Me	167°	167°
NC <sup>α</sup> CO	324°	324°

The kinetic rates are of the same order of magnitude of those reported for YbDOTA by Jacques and Desreux.<sup>[6]</sup> In the present case, however, only one process is observed, linked to the inversion of the macrocyclic ring. Apparently, the rotation of the methyl acetate arm is strongly hindered, by analogy with what observed in some LnDOTA analogues.<sup>[13][33]</sup> The detailed comparison with the kinetic rates of DOTA is not straightforward, owing to the different molar ratios of the forms in the two complexes. The averages of the direct to reverse rates of ring inversion at 25°, weighted for the two populations, gives 44.8 s<sup>-1</sup> for YbDOTA<sup>[8][21]</sup> and 12.5 s<sup>-1</sup> for YbDOTMA. The dynamics of the latter is probably slowed down by the crowding due to the presence of the methyl on the side branches.

The thermodynamic data for the interconversion process show both negative enthalpy and entropy. Apparently, the minor form is slightly more stable and only entropically unfavoured. The loss of entropy in the process D → d indicates that in this conversion the order of the system increases, which is compatible with a different coordination number of the central cation, that should be larger for the minor form. Aime et al.<sup>[8]</sup> reported that on going from the major to the minor form of YbDOTA,  $\Delta H^\circ = +17.5$  kJ mol<sup>-1</sup> and  $\Delta S^\circ = +45$  J K<sup>-1</sup> mol<sup>-1</sup> and they attributed the large and *positive* entropy change to the release of a water molecule, axially coordinated in the former. This hypothesis is also strongly supported by variable-pressure NMR. Since the reaction entropy is rather similar to that found for the conversion m' → M in DOTA,<sup>[8]</sup> it seems quite reasonable to extrapolate this result to DOTMA, where the major form should be eight coordinate and the minor form should be hydrated and nine coordinate; this further con-

sideration is in agreement with the assignment of an M-type structure ( $n$  diastereomer) to the minor isomer, where the metal ion is less hindered.

## Conclusions

Pseudocontact shifted  $^1\text{H-NMR}$  spectra of YbDOTMA have demonstrated that in solution two forms are present which exchange slowly and are, in principle, both compatible with the same set of geometrical factors for the protons. Two-dimensional EXSY spectra, on the other side, show that the two forms correspond to different conformations of the macrocyclic ring, in diastereomeric relation, as  $p$  or  $n$  forms. This is in close analogy with DOTA derivatives.<sup>[8][33]</sup> Only steady-state NOE spectra, however, indicate the geometry of the major isomer, thus finally solving the problem of the structural assignment of this molecule in solution in a fully consistent way and without reference to crystal structures. While three different equilibria could be observed for YbDOTA, in the temperature range examined in this work only one has been detected between the two YbDOTMA species, since the presence of the methyl group in the acetate side arms enhances the conformational homogeneity of the chelate system, constraining the arrangement of the pendant groups and favouring one conformation of the cycle ethylene groups.

The steric hindering affects the kinetic parameters, too, and quantitative EXSY measurements show that the ring inversion is slowed down with respect to the corresponding process in YbDOTA. The thermodynamic parameters of the equilibrium indicate that the structural rearrangement may be accompanied by a hydration process. The relative populations of the two forms and the hydration–dehydration dynamics are in reverse analogy with YbDOTA.<sup>[33]</sup>

It is noteworthy that the two species in equilibrium are  $\Lambda(\lambda\lambda\lambda\lambda)$  and  $\Lambda(\delta\delta\delta\delta)$ , thus characterized by the same helicity about the metal cation. One can therefore conclude that, by analogy with other chiral ligands,<sup>[11–13]</sup> YbDOTMA shows a transfer of chirality from a local stereogenic element to the overall structure. This is a key point in understanding the stereochemistry and consequently the chiroptical properties of these complexes

## Experimental Section

**General:** The anionic homochiral and enantiopure YbDOTMA complex as a methylglucammonium salt was a gift from Bracco Italy S.p.A. and was dissolved in  $\text{D}_2\text{O}$  (21.8 mg in 0.5 mL, 52.80 mM) and MeOD (6.95 mg in 0.5 mL, 16.83 mM). The NMR spectra were recorded on a Varian VXR 300 Spectrometer operating at 7.1 T, equipped with a VT unit stable within 0.1 °C. Where not otherwise specified, the temperature was 25 °C. The 90° pulse length was 14.5  $\mu\text{s}$ . The recycle delay in all experiments was above 0.5 s, largely exceeding 5  $T_1$  of all YbDOTMA proton resonances and ensuring instrumental recovery. – Steady-state NOE spectra were recorded with 4096 transients after 0.5 s with cw pre-saturation of the relevant signals. – EXSY spectra were recorded

with the standard NOESY sequence, using the hypercomplex method to obtain phase sensitivity in both dimensions. Since zero quantum coherences have an antiphase character, they cannot contribute neither in integrated nor in point amplitude in systems with a linewidth largely exceeding the scalar couplings; thus no attempt was made to suppress them. 2048 points were collected for each of the 512  $t_1$  increments, covering a spectral window of 50000 Hz in two dimensions. The matrices were zero-filled to 2 K  $\times$  2 K and weighted by Lorentz-to-Gauss functions in both dimensions. Since all quantitative analyses were performed only on the methyl resonances (within 12000 Hz from the transmitter), no correction for finite pulse length was used. No baseline correction was applied and the 1- and 2-dimensional integrals were evaluated with the VNMR software with reference to the area immediately adjacent to each peak. The pseudocontact shifts were calculated with reference to the data reported for LuDOTA.<sup>[4]</sup> The geometric factors for the protons were calculated with the aid of standard molecular modelling software.<sup>[23]</sup> In the first place, only the four cyclen-proton resonances were considered: a tentative value for  $D$  was obtained, through which starting values for the geometric factors of the acetate and the methyl protons were assessed. The dihedral angle about the N–C $^\alpha$  bond was systematically varied in order to approach those values. This procedure revealed that only one minimum could be found. Thereupon, for values of the dihedral YbNC $^\alpha$ M between 165° and 170°, all the geometric factors and pseudocontact shifts were included in the linear fitting, seeking for the best agreement factor.<sup>[24]</sup> –  $^1\text{H-NMR}$  spectrum at 300 MHz of YbDOTMA in  $\text{D}_2\text{O}$  and in MeOD (Figure S1), correlation plot between the experimental  $\delta^{\text{exp}}$  values and the geometrical factors calculated for YbDOTMA in  $\text{D}_2\text{O}$  (Figure S2), variable temperature behavior (from 25 to –80 °C) of the methyl resonances of YbDOTMA (Figure S3), NOE difference spectra of YbDOTMA obtained upon saturation of the acetate C resonance of the major form (Figure S4) are available as supporting Information.

## Acknowledgments

We thank Bracco Italy S.p.A. for a generous gift of YbDOTMA.

[1] Abbreviated names for this and the other compounds are DOTA = 1,4,7,10-tetraazacyclododecane-1,4,7,10-tetraacetic acid, DOTMA = (1*R*,4*R*,7*R*,10*R*)- $\alpha,\alpha',\alpha'',\alpha'''$ -tetramethyl-1,4,7,10-tetraazacyclododecane-1,4,7,10-tetraacetic acid, DOTAM = 1,4,7,10-tetrakis(2-carbamoyl-ethyl)-1,4,7,10-tetraazacyclododecane, THP = 1,4,7,10-tetrakis(2-hydroxypropyl)-1,4,7,10-tetraazacyclododecane, DOTPBz $_4$  = 1,4,7,10-tetraazacyclododecane tetrakis(methylenebenzylphosphinic acid), DO3MA = (1*R*,4*R*,7*R*)- $\alpha,\alpha',\alpha'''$ -trimethyl-1,4,7,10-tetraazacyclododecane-1,4,7-triacetic acid, Parker's phenylethylamide = 1,4,7,10-tetrakis[(*R*)-1-(phenyl)ethylcarbamoylmethyl]-1,4,7,10-tetraazacyclododecane, Parker's naphthylethylamide = 1,4,7,10-tetrakis[(*R*)-1-(1-naphthyl)ethylcarbamoylmethyl]-1,4,7,10-tetraazacyclododecane.

[2] J. F. Desreux, *Inorg. Chem.* **1980**, *19*, 1319–1324.

[3] M. R. Spirllet, J. Rebizant, J. F. Desreux, M. F. Loncin, *Inorg. Chem.* **1984**, *23*, 359–363.

[4] S. Aime, M. Botta, G. Ermondi, *Inorg. Chem.* **1992**, *31*, 4291–4299.

[5] J.-P. Dubost, M. Legar, D. Meyer, M. Schaefer, *C. R. Acad. Sci. Paris, Ser. 2* **1991**, *312*, 349–354.

[6] V. Jacques, J. F. Desreux, *Inorg. Chem.* **1994**, *33*, 4048–4053.

[7] S. Aime, A. Barge, M. Botta, M. Fasano, J. D. Ayala, G. Bombieri, *Inorg. Chim. Acta* **1993**, *246*, 423–429.

[8] S. Aime, M. Botta, M. Fasano, M. P. M. Marques, C. F. G. C. Galdes, D. Pubanz, A. E. Merbach, *Inorg. Chem.* **1997**, *36*, 2059–2068.

[9] S. Aime, A. Barge, F. Benetollo, G. Bombieri, M. Botta, F. Uggeri, *Inorg. Chem.* **1997**, *36*, 4287–4289.

- [10] H. G. Brittain, J. F. Desreux, *Inorg. Chem.* **1984**, *23*, 4459–4466.
- [11] R. S. Dickins, J. A. K. Howard, C. W. Lehmann, J. Moloney, D. Parker, R. Peacock, *Angew. Chem. Int. Ed. Engl.* **1997**, *36*, 521–523.
- [12] R. S. Dickins, J. A. K. Howard, J. Moloney, D. Parker, R. Peacock, G. Siligardi, *J. Chem. Soc., Chem. Commun.* **1997**, 1747–1748.
- [13] J. A. K. Howard, A. M. Kenwright, J. M. Moloney, D. Parker, M. Port, M. Navet, O. Rousseau, M. Woods, *J. Chem. Soc., Chem. Commun.* **1998**, 1381–1382.
- [14] S. Aime, M. Botta, M. Fasano, E. Terreno, P. Kinchesh, L. Calabi, L. Paleari, *Magn. Reson. Med.* **1996**, *35*, 648–651.
- [15] M. F. Tweedle, K. Kumar, R. B. Shukla, R. Ranganathan, S. Aime, M. Botta, J. Di Marco, Z. Gougoutas, *Book of Abstracts, 23th International Symposium on Macrocyclic Chemistry*, Turtle Bay, Hawaii, **1998**.
- [16] S. Aime, M. Botta, G. Ermondi, P. L. Anelli, F. Fedeli, F. Uggeri, *Proceedings, SMR, 2nd Annual Meeting*, San Francisco, **1994**.
- [17] L. Di Bari, G. Pintacuda, P. Salvadori, *Book of abstracts, 6th International Conference on Circular Dichroism*, Pisa, Italy, **1997**; L. Di Bari, G. Pintacuda, P. Salvadori, *Book of abstracts, 24th FGIPS Meeting in Inorganic Chemistry*, Corfu, Greece, **1997**; G. Pintacuda, L. Di Bari, P. Salvadori, *Book of abstracts, 23th International Symposium on Macrocyclic Chemistry*, Turtle Bay, Hawaii, **1998**.
- [18] J. R. Morrow, S. Amin, C. H. Lake, M. R. Churchill, *Inorg. Chem.* **1993**, *32*, 4566–4572.
- [19] K. O. A. Chin, J. R. Morrow, C. H. Lake, M. R. Churchill, *Inorg. Chem.* **1994**, *33*, 656–664.
- [20] S. Aime, A. S. Batsanov, M. Botta, J. A. K. Howard, D. Parker, K. Senanayake, G. Williams, *Inorg. Chem.* **1994**, *33*, 4696–4706.
- [21] S. Hoefft, K. Roth, *Chem. Ber.* **1993**, *126*, 869–873.
- [22] We prefer to borrow the stereochemical descriptors *n* and *p*, which clarify the diastereomeric nature of the rearranged forms, and avoid reference to the major form of YbDOTA. Indeed, the structures of the predominant form in solution depend on the nature of the ligand and on the size of the central ion.
- [23] All the operations on the structures described can be performed with a standard molecular modelling package, such as *Hyperchem* (Hypercube Inc.) or *CS ChemDraw Pro* (CambridgeSoft Corporation).
- [24] The agreement factor *R* between calculated,  $\delta_s(\text{calcd.}, i)$ , and experimental,  $\delta_s(\text{exp.}, i)$ , pseudocontact shifts, defined as:
- $$R^2 = \frac{\sum_i (\delta_i^{\text{calc}} - \delta_i^{\text{exp}})^2}{\sum_i (\delta_i^{\text{exp}})^2}$$
- is reported in Table 1, as well. We can observe that, even if the *R* value for the major isomer is slightly lower, the agreement is very good for both structures. Variation of the torsion around the N–C $\alpha$  bond by 5° about the optimal value does not imply a relevant increase of the factor, *R* (about 10% higher when the angle is 170°).
- [25] The geometrical factors calculated on the basis of the published of GdDOTA (ref.<sup>[5]</sup>) lead to the assignment shown in ref.<sup>[6]</sup>, featuring the two protons on each macrocycle carbon bearing different numbers. This is in agreement with that reported by several authors (ref.<sup>[6]</sup><sup>[21]</sup>), but in contrast with Aime and co-workers (ref.<sup>[4]</sup><sup>[15]</sup>).
- [26] S. Aime, M. Botta, S. Geminiatti Crich, E. Terreno, P. L. Anelli, F. Uggeri, *Chem. Eur. J.* **1999**, *5*, 1261–1266.
- [27] B. Bleaney, *J. Magn. Reson.* **1972**, *8*, 91–100.
- [28] For a general reference on the NMR of paramagnetic molecules, see: I. Bertini, C. Luchinat, *Coord. Chem. Rev.* **1996**, *150*, 1–296.
- [29] C. L. Perrin, R. K. Gipe, *J. Am. Chem. Soc.* **1984**, *106*, 4036–4038.
- [30] E. W. Abel, T. P. J. Coston, K. G. Orrell, V. Sik, D. Stephenson, *J. Magn. Reson.* **1986**, *70*, 34–53.
- [31] The errors on these values were estimated through their dispersion for the various experiments.
- [32] The NOE between A<sub>2</sub> and C is not diagnostic, since in both structures  $\Lambda(\delta\delta\delta\delta)$  and  $\Lambda(\lambda\lambda\lambda\lambda)$  the two protons are nearby. Furthermore, it is very difficult to detect, owing to the large relaxation rates of the two nuclei, which sit close to the paramagnetic centre.
- [33] S. Aime, M. Botta, G. Ermondi, E. Terreno, P. L. Anelli, F. Fedeli, F. Uggeri, *Inorg. Chem.* **1996**, *35*, 2726–2736.

Received April 22, 1999  
[199141]